Origin of Laurdan Sensitivity to the Vesicle-to-Micelle Transition of Phospholipid-Octylglucoside System: A Time-Resolved Fluorescence Study

Mathias Viard,* Jacques Gallay,[†] Michel Vincent,[†] and Maïté Paternostre*

*Equipe Physicochimie des Systèmes Polyphasés, Université Paris Sud, FR-92296 Châtenay Malabry, and [†]L.U.R.E., Université Paris Sud, FR-91 Orsay, France

ABSTRACT   The fluorescent probe laurdan has been shown to be sensitive to the vesicle-to-micelle transition of phosphatidylcholine/octylglucoside (M. Paternostre, O. Meyer, C. Grabielle-Madelmont, S. Lesieur, and M. Ollivon, 1995, *Biophys. J.* 69:2476–2488). On the other hand, a study on the photophysics of laurdan in organic solvents has shown that the complex de-excitation pathway of the probe can be described by two successive processes, i.e., an intramolecular charge transfer followed by dielectric relaxation of the solvent if polar. These two excited-state reactions lead to three emitting states, i.e., a locally excited state, a charge transfer state, and a solvent relaxed state (M. Viard, J. Gallay, M. Vincent, B. Robert and M. Paternostre, 1997, *Biophys. J.* 73:2221–2234). Experiments have been performed using time-resolved fluorescence on the probe inserted in amphiphile aggregates (mixed liposomes, mixed micelles) different in detergent-to-lipid ratios. The results have been compared with those obtained for laurdan inserted in dipalmitoyl phosphatidylcholine liposomes in the gel and in the fluid lamellar phase. Except for laurdan in dipalmitoyl phosphatidylcholine liposomes in the gel lamellar phase, the red part of the emission spectra originates from the de-excitation of the relaxed excited state of laurdan, indicating that indeed the dielectric relaxation process is an important phenomena in the ground-state return pathway of this probe. On the other hand, the maximization entropy method (MEM) analysis of the fluorescence decay recorded in the blue part of the emission spectra indicates that the dielectric relaxation is not the only reaction occurring to the excited state of laurdan. Moreover, the analysis of the fluorescence decays of laurdan inserted in gel lamellar dipalmitoylphosphatidylcholine (DPPC) liposomes indicates excited-state reactions, although dielectric relaxation is impossible. These results are in agreement with the de-excitation pathway determined from laurdan behavior in organic solvent even if, in most of the aggregates studied in this work, the major phenomenon is the dielectric relaxation of the solvent. All along the vesicle-to-micelle transition, we have observed that the lifetime of the relaxed excited state of laurdan continuously decreases probably due to a dynamic quenching process by water molecules. On the other hand, the time constant of the dielectric relaxation process remains almost unchanged in the lamellar part of the transition but abruptly decreases as soon as the first mixed micelle is formed. This decrease is continuous all over the rest of the transition even if it is more pronounced in the mixed liposomes' and mixed micelles' coexistence. The increase of the octylglucoside-to-lipid ratio of the mixed micelles via the change of the size and the shape of the aggregates may facilitate the penetration and the mobility of water molecules. Therefore, during the vesicle-to-micelle transition, laurdan probes the evolution of both the amphiphile packing in the aggregates and the increase of the interface polarity. This study finally shows that the detergent-to-lipid ratio of the mixed micelles is an important parameter to control to limit the penetration and the mobility of water within the amphiphile aggregates and that laurdan is a nice tool to monitor this phenomenon.

INTRODUCTION

The study of a membrane protein often requires its reconstitution in an artificial lipid bilayer, i.e., the extraction of the protein from the natural membrane and its incorporation in a perfectly defined (lipid composition, protein density, and protein orientation) artificial one (Sylvius, 1992; Paternostre et al., 1988; Rigaud et al., 1988). Solubilization and purification is also a prerequisite for membrane protein crystallization (Garavito et al., 1996). Detergents are used to solubilize biological membranes and, via the detergent removal, the reconstitution of artificial lipidic bilayers mimicking the original one can be achieved. However, the

control of this procedure depends on the knowledge of the intermediary structures that appear during the solubilization and the reconstitution processes. Many efforts have been devoted to understand the interactions between detergents and phospholipids or the so-called vesicle-to-micelle transition. Although numerous studies have been performed on this transition (Helenius and Simons, 1975; Ollivon et al., 1988; Lichtenberg et al., 1983; Lichtenberg, 1996; Rigaud et al., 1995; Paternostre et al., 1995), the molecular and the supramolecular mechanisms are still not fully understood from a physicochemical point of view. Indeed, even if the transition can easily be defined at each boundary by the molecular composition of the mixed aggregates and by the detergent concentration in its monomer form in equilibrium, the organization, the structure, and the morphology of the intermediate aggregates as well as their interface properties are not yet fully elucidated.

Fluorescent probes are frequently used to study the structure and the dynamic of biological systems such as proteins,

membranes, or nucleic acids. The techniques based on fluorescence allow the study of the interactions taking place between the fluorophore excited state and its environment. The excited-state lifetime depends on the environment and is in a picosecond to nanosecond range, allowing the study of phenomena arising in this time period. Moreover, the interaction of the probe excited state with its environment induces changes in the ground state return pathway. The sensitivity of the probe to the polarity of the environment is related to the extent of the dipole moment created after light absorption. To gain in sensitivity, Weber and Farris designed a probe that includes a donor and an acceptor group substituted at the opposite of a naphthalene ring: 6-propionyl-2-(dimethylamino)naphthalene (prodan) allowing the appearance of a large dipole moment (8 Debye; Balter et al., 1988). Prodan has been used for various studies on biomembranes (Chong, 1988; Chong et al., 1989; Zeng and Chong, 1991; Rottenberg, 1992). However, prodan being only anchored to the lipid bilayer by a small aliphatic chain, it partitions between the water and the membrane complicating the interpretation of the results. New probes carrying a similar fluorophore group but varying the amino group or the aliphatic chain were synthesized to gain in selectivity. Different probes were designed, such as danca, which exhibits a specific affinity for the myoglobin heme (Cowley, 1986), patman, or laurdan. These last two include a long aliphatic chain (C_{12}) by which the probe is maintained in phospholipid membranes and the fluorophore itself stays at the level of the glycerol backbone (Chong and Wong, 1993). This strong anchorage considerably limits the exchange of the probe with the aqueous media.

In particular, laurdan has then been extensively used by Parasassi and colleagues to characterize the gel to fluid phase transition in phospholipid membranes (Parasassi et al., 1986a,b, 1990, 1991; Parasassi and Gratton, 1992) and to detect the phase separation domains generated by the presence of cholesterol (Parasassi et al., 1994a,b, 1995). This probe has also been shown to be sensitive to the vesicle-to-micelle transition induced by the addition of detergent to a liposome suspension. Laurdan allowed notably the determination of the partitioning of the detergent between water and lipid aggregates along the transition and especially in the mixed micellar domain (Heerklotz et al., 1994; Paternostre et al., 1995). The origin of the sensitivity of this probe to the different phenomena is, however, not completely understood.

The photophysics of this probe may correspond to the three-step model recently proposed (Viard et al., 1997). It has been shown by studying the fluorescence properties of laurdan dissolved in either nonpolar and viscous solvents or in ethanol as a function of temperature that a two-step model cannot entirely describe the de-excitation of laurdan. Indeed a very fast rate has been evidenced between the locally excited state (LE) and the so-called charge transfer (CT) excited state, this last CT state undergoing when possible a dipolar relaxation process of the solvent leading to another emitting state, i.e., a solvent relaxed excited state.

In the following, we have performed time-resolved fluorescence experiments to determine the fluorescence decays of laurdan inserted in different amphiphile aggregates formed during the vesicle-to-micelle transition. From previous studies, we know that the fluorescence of laurdan is very sensitive to the water relaxation process occurring at the water-amphiphile interface (Parasassi et al., 1991). One of the aims of this study was to gain information about the evolution of the interface of the amphiphile aggregates during the vesicle-to-micelle transition induced by octylglucoside (OG). This study also allowed us to test the three-step model proposed in our previous study for the laurdan de-excitation process.

MATERIALS AND METHODS

Laurdan was purchased from Molecular Probes (Eugene, OR). Egg-phosphatidylcholine (EPC) was obtained from Avanti Polar Lipids (Birmingham, AL), and egg-phosphatidic acid (EPA) and octylglucoside (OG) were from Sigma Chemical Co. (St. Louis, MO). All of these products were used without further purification.

Liposome preparation

Liposomes were prepared either by reverse-phase evaporation followed by extrusion through calibrated filters as described by Lesieur et al. (1993) for EPC/EPA liposomes or by sonication for dipalmitoylphosphatidylcholine (DPPC) liposomes (Schullery et al., 1980). The liposomes were formed in an aqueous buffer containing 10 mM HEPES, 145 mM NaCl , pH 7.4.

For EPC/EPA liposomes (90/10% mol/mol), laurdan (0.1% mol/mol of the total lipid contents) was mixed in the presence of chloroform. The lipids were dried under nitrogen and lyophilized overnight. After reverse-phase evaporation (Szoka and Papahadjopoulos, 1978), the liposomes were sequentially extruded through Nucleopore filters of 0.8, 0.4, 0.2, 0.1, and 0.05 μm in pore diameters to form large unilamellar vesicles, uniform in size and ~120 nm in diameter at the end of the extrusion procedure as measured by dynamic light scattering.

For DPPC liposomes containing 0.1% of laurdan a procedure similar to that designed for EPC/EPA mixtures was used to dry the lipids. After hydration of the dried lipids, six cycles of sonication of 3 min each using a Branson sonicator was applied to the lipid suspension maintained at 50°C. After sonication the liposome preparation was centrifuged (10000 rpm for 10 min) to remove the titanium particles coming from the sonication probe. The sample was then kept at room temperature, and during the first few hours the size increased from ~40 to 80 nm as measured by dynamic light scattering.

Monitoring of the solubilization process by turbidity and fluorescence measurements

The solubilization of EPC/EPA vesicles containing laurdan at 25°C was monitored by measuring simultaneously the turbidity at 350 nm and the fluorescence at two emission wavelengths (435 and 500 nm) on a Fluoromax fluorimeter (Spex Instruments, Jobin Yvon, Longjumeau, France) equipped with four photomultipliers and connected to a computer (Paternostre et al., 1995). During the continuous addition of OG into a cuvette containing the initial laurdan-labeled liposomes (either EPC/EPA or DPPC liposomes) maintained under magnetic stirring, the turbidity and fluores-

cence signal were recorded versus time. The rate of addition of OG was monitored by a syringe pump and kept constant all along the experiment, allowing us to deduce from the time the final OG concentration in the cuvette by using the following equation:

$$[OG]_t = ([OG]_s r_s t)/(V_o + (r_s t)), \qquad (1)$$

in which $[OG]_t$ and $[OG]_s$ are the OG concentration in the cuvette and in the syringe, respectively, V_o is the initial volume of the liposome suspension in the cuvette, r_s is the rate of OG addition in ml/s, and t is the time measured in seconds. The evolution of both the turbidity of the suspension and the fluorescence intensity ratio (I_{500}/I_{435}) was plotted against the OG concentration.

Steady-state fluorescence spectra

The steady-state fluorescence spectra were measured using a photon-counting Fluoromax fluorimeter (Spex Instruments), and correction for monochromators and source-dependent variation intensity were systematically performed.

Steady-state emission spectra (λ_{exc} = 360 nm and 400 < λ_{em} < 600 nm) have been recorded for laurdan-containing DPPC liposomes during a continuous increase of temperature. For this type of experiment, the temperature of the cuvette was controlled via a cryostat (RC6, Lauda, Germany) and the temperature was controlled within the cuvette using a thermocouple (Ni/Cr-Ni/Al). The cryostat was monitored by an external homemade system allowing a linear temperature increase between 15°C and 65°C at a rate of 0.11°C/min. Emission spectra were recorded continuously during this temperature increase. In these experimental conditions, the variation of temperature between the beginning and the end of one spectrum was constant (Δt = 0.35°C).

Fluorescence lifetime measurements

Fluorescence intensity decays were obtained by the time-correlated single-photon-counting technique from the polarized components $I_{vv}(t)$ and $I_{vh}(t)$ on the experimental setup installed on the SB1 beam line of the synchrotron radiation machine Super-ACO (L.U.R.E., Orsay, France), which has been described elsewhere (Vincent et al., 1995a,b). The light pulse has a full width at half maximum of ~500 ps at a frequency of 8.33 MHz for a double bunch mode.

Data for I_{vv} and I_{vh} were stored in separated 2-kilobit memories. The instrumental response function was automatically recorded each 5 min by measuring the scattering of a glycogen solution during 30 s at the emission wavelength in alternation with the parallel and perpendicular component of the polarized fluorescence decay, which were cumulated during 90 s. The time resolution was in the range of 7 to 25 ps per channel depending on the experiments. The shortest excited-state lifetime the instrument is able to resolve has values of 50 ps. For low-temperature measurements a Janis cryostat was used (Vincent et al., 1995a,b; Viard et al., 1997).

Data analysis of fluorescence decays

Analysis of the fluorescence intensity decay data was performed by the maximum entropy method (MEM) (Livesey and Brochon, 1987). The program uses MEMSYS 5 as a library of subroutines. Optionally, MEMSYS 5 can handle a 150-dimensioned vector without any a priori assumption on each of the amplitude signs (Vincent et al., 1995a,b). This option was used when the classical analysis with only positive amplitudes did not provide good results in terms of χ^2 values and shape of the plot of the weighted residuals.

Because polarized light was used in these experiments, the total intensity decay $T(t)$ is built by adding the parallel (I_{vv}) and twice the perpendicular components (I_{vh}) according to Eq. 2. The correction factor β_{corr}

takes into account the difference of transmission of the polarized light components by the optics:

$$T(t) = I_{vv}(t) + 2\beta_{corr}I_{vh}(t) \qquad (2)$$

$$T(t) = E_\lambda(t)* \int_0^\infty \alpha(\tau)\exp(-t/\tau)d\tau, \qquad (3)$$

where $E_\lambda(t)$ is the temporal shape of the excitation light pulse, the asterisk denotes a convolution product, and $\alpha(\tau)$ is the lifetime distribution given by

$$\alpha(\tau) = \int_0^\infty \int_{-0.2}^{0.4} \gamma(\tau, \theta, A)d\theta dA. \qquad (4)$$

The recovered distribution $\alpha(\tau)$, which maximizes the entropy function S, is chosen:

$$S = \int_0^\infty \left\{ \alpha(\tau) - m(\tau) - \alpha(\tau)\log\left[\frac{\alpha(\tau)}{m(\tau)}\right] \right\}d\tau \qquad (5)$$

In this expression, $m(\tau)$ is the starting model. In every analysis, a flat map over the explored (τ) domain was chosen for $m(\tau)$, as no a priori knowledge about the final distribution was available. The analysis was bound by the χ^2 constraint:

$$\sum_{k=1}^{M} \frac{(I_k^{calc} - I_k^{obs})^2}{\sigma_k^2} \leq M, \qquad (6)$$

where I_k^{calc} and I_k^{obs} are the kth calculated and observed intensities. σ_k^2, the variance of the k point, is equal to $\sigma_{k,vv}^2 + 4\beta_{corr}^2 * \sigma_{k,vh}^2$ (Wahl, 1979). M is the total number of observations.

The center $\langle\tau_j\rangle$ of a single class j of lifetimes and its associated contribution C_j were defined, respectively, as

$$\langle\tau_j\rangle = \sum_i \alpha(\tau_i)\tau_i \qquad (7)$$

and

$$C_j = \sum_i \alpha(\tau_i), \qquad (8)$$

the summation being performed on the interval defining this j class, with $\Sigma_{i=1}^{i=n} \alpha(\tau_i) = 1$ (n is the total number of lifetimes used in the analysis, routinely taken as 150).

Time-resolved fluorescence emission spectra (TRES): collection and analysis

TRES were reconstructed from individual decays recorded at different wavelengths to cover all the emission spectra (bandwidth between 2 and 10 depending on the experiments). Each individual decay was fit with the MEM program using the classical or the negative amplitude option. The integral of each decay curve was normalized to the corresponding steady-state fluorescence emission wavelength recorded on the same instrument with identical experimental conditions. By collecting the vertical (I_{vv}) and the horizontal (I_{vh}) fluorescence intensity components and by taking into account the β_{corr} correction factor, the calculated impulse fluorescence intensity (Eq. 4) as well as the steady-state intensity ($I_{vv} + 2\beta_{corr}I_{vh}$) are de

facto corrected for the difference of transmission of the polarized light components by the optics. For the quantitative description of the spectral shift, the barycenters in frequency were computed and the full widths at half peak were calculated from the raw spectra. The shift function $C(t)$ was defined classically as (Bagchi, 1989)

$$C(t) = \frac{\bar{v}_t - \bar{v}_\infty}{\bar{v}_0 - \bar{v}_\infty}, \tag{9}$$

where $\bar{v}_t$, $\bar{v}_0$, and $\bar{v}_\infty$ are the barycenter values in frequency at time t, 0, and ∞, respectively. Reaction rate constants (τ_{rj}) were determined from the analysis of $C(t)$ as a sum of exponentials with MEM (Vincent et al., 1995a,b):

$$C(t) = \sum_j a_j e^{-t/\tau Rj} \tag{10}$$

RESULTS
Evolution of the fluorescence emission spectra of laurdan during the vesicle-to-micelle transition

The emission spectrum of laurdan is sensitive to the vesicle-to-micelle transition. As shown on Fig. 1 *A*, the solubilization by OG of large EPC/EPA unilamellar liposomes containing 0.1% (mol/mol) laurdan leads to a decrease of the blue part of the emission spectrum, compared with the red part, and to a red shift of the emission maximum.

The solubilization process can therefore be followed, during the addition of OG into a cuvette containing the initial liposomes suspension, through the evolution of the fluorescence intensity ratio I_{510}/I_{434} (Fig. 1 *B*, curve b). The evolution of the turbidity at 350 nm can also be measured simultaneously (Fig. 1 *B*, curve a). According to the literature (Paternostre et al., 1995), the two dashed lines (Fig. 1 *B*) delimit the lamellar, the mixed lamellar-micellar, and the micellar domains of the vesicle-to-micelle transition. The evolution of the fluorescence intensity ratio of laurdan during the solubilization process points out that the emission spectrum of laurdan is greatly affected as soon as the first micelles are formed whereas only slight modifications are seen in the lamellar domain of the transition. We have undertaken time-resolved fluorescence experiments on laurdan inserted in different OG-lipid aggregates situated in the lamellar (Fig. 1 *B*, samples 1 to 3), in the mixed lamellar-micellar (Fig. 1 *B*, sample 4), and in the micellar part (Fig. 1 *B*, samples 5 to 13) of the solubilization process.

Evolution of the fluorescence decays of laurdan during the vesicle-to-micelle transition

In this section the experiments presented were carried on the samples 1 to 5 selected on the basis of the solubilization curves visualized either by turbidity or fluorescence measurements (Fig. 1 *B*). For each sample, the fluorescence decays have been recorded for emission wavelengths situated in the blue edge (λ_{em} = 408 nm) and in the red edge (λ_{em} = 550 nm) of the spectrum and for a constant excita-
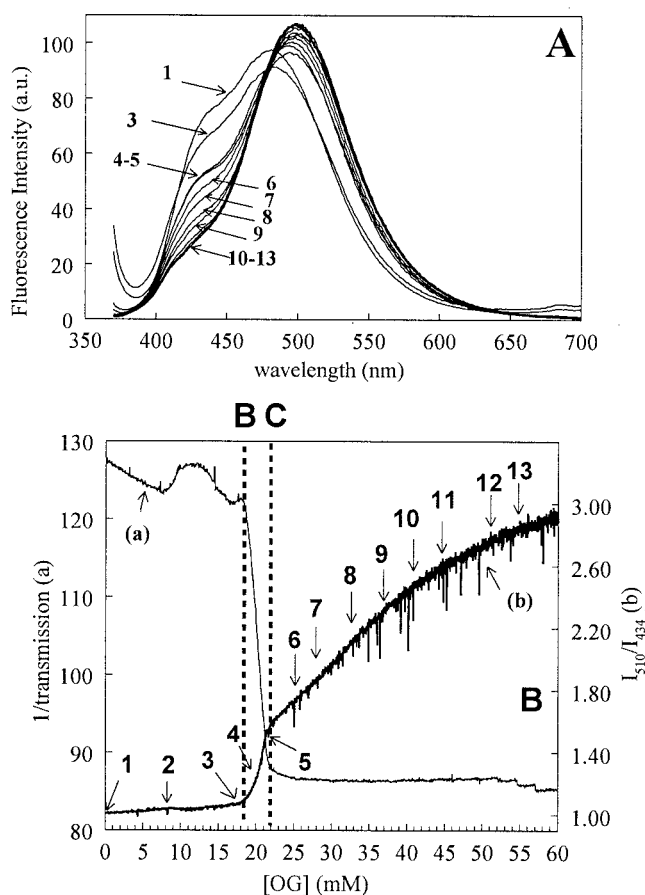

FIGURE 1   (*A*) Evolution of the emission spectra of laurdan (λ_{exc} = 360 nm) during the solubilization of EPC/EPA liposomes ([lipid]$_0$ = 2 mM) by OG. The areas of the spectra were normalized. (*B*) Evolution of the turbidity (*curve a*) and the fluorescence intensity ratio (I_{490}/I_{435}; *curve b*) during the solubilization of initially laurdan-labeled liposomes by OG. The arrows from 1 to 13 indicate the samples that have been further studied by time-resolved fluorescence ([lipid]$_0$ = 2 mM). The dashed lines indicate the points B and C of the transition and delimit the three domains of the vesicle-to-micelle transition (lamellar before point B, coexistence of lamellar/mixed micellar between points B and C, and mixed micellar after point C).

tion wavelength of 360 nm. The fluorescence decays were analyzed by the MEM, and the results are reported in Fig. 2.

For the decays recorded in the red edge of the emission spectrum and whatever the type of aggregate in which laurdan is inserted, essentially two lifetime distributions in the nanosecond range are determined by the MEM analysis and their amplitudes are opposite in sign (Fig. 2). According to Viard et al. (1997), the two lifetime distributions correspond to the rate constant of the dipolar relaxation process (the shortest time distribution associated with a negative amplitude) on the one hand and to the lifetime of the relaxed excited state (the longest time distribution associated with a positive amplitude) on the other hand. In Fig. 3 we have reported the time constant of the solvent relaxation process (T_{rel}) and the lifetime of the relaxed state (τ_{rel}) as a function
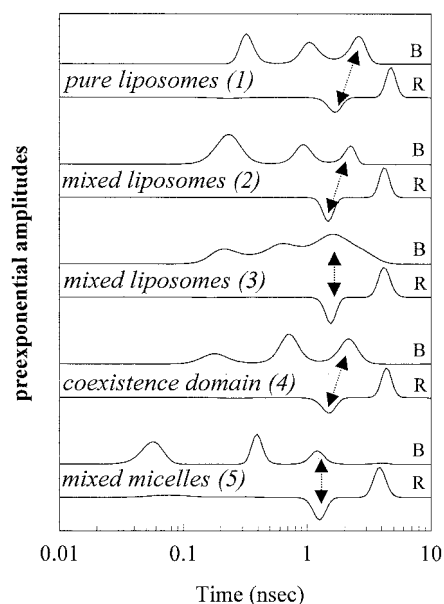
FIGURE 2   Results of the MEM analysis of the fluorescence decays recorded for laurdan inserted in the mixed aggregates indicated on Fig. 1 *B* by the arrows 1 to 5. For each sample, the upper trace is the analysis of the fluorescence decay recorded in the blue edge of the emission spectra ($\lambda_{blue} = 408$ nm), whereas the lower trace is the analysis obtained for the fluorescence decay recorded in the red edge of the spectra ($\lambda_{red} = 550$ nm). The excitation wavelength was fixed at 360 nm for all the samples, and the temperature was kept constant at 20°C. The dashed arrows indicate the time distribution found similar in the MEM analysis of the blue and the red decays.

FIGURE 3   Rate constant distributions obtained from the MEM analysis of the fluorescence decays recorded for red emission wavelengths. τ_{rel} (●) is the lifetime of the excited relaxed state and T_{rel} (▲) the time constant of the dielectric relaxation process corrected according to the following equation (Vincent et al., 1995a,b): $1/t_{rel} = 1/T_{rel} + 1/\tau_{rel}$, where t_{rel} is the time constant determined by the MEM analysis. The vertical dashed lined indicates the points B and C of the vesicle-to-micelle transition (cf. Fig. 1 *B*). The open symbols represent τ_{rel} (○) and T_{rel} (△) for laurdan inserted in pure OG micelles (PM).

of the total OG concentration in the solution. In the first part of the transition, i.e., the lamellar domain (until the first vertical dashed line), τ_{rel} slightly decreases whereas T_{rel} remains almost constant. On the other hand, in the mixed lamellar-micellar domain (between the two dashed lines), T_{rel} abruptly decreases from 2.4 to 1.9 ns. This significant acceleration of the solvent relaxation process occurs as soon as the first mixed micelles are formed.

For the decays recorded in the blue edge of the emission spectrum, the results of the MEM analysis are complex: three to four lifetime distributions all associated with positive amplitudes are observed. This result indicates that the probe undergoes a succession of reactions at the excited state before de-excitation. Some of these lifetime distributions might be related to those present on the analysis of laurdan decays recorded in the red edge. For example, one of the longest lifetime distributions determined for the decays recorded in the blue edge of the spectrum is similar to the rate constant of the solvent relaxation rate constant (dotted arrows in Fig. 2). On the other hand, the lifetime of the relaxed state is almost invisible on the decay recorded on the blue edge of the emission spectra, except for the mixed micelles for which a distribution with very weak amplitude is determined from the MEM analysis at ~4 ns. For the other lifetime distributions determined from the
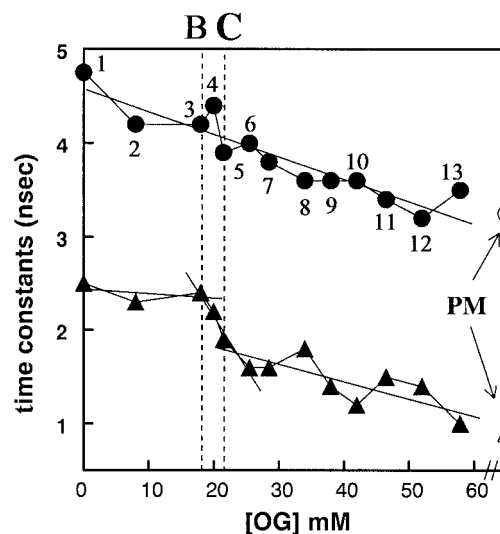
MEM analysis of the decays recorded in the blue edge of the spectrum no equivalence with the analysis of the decays recorded in the red edge can be found. The MEM analyses of these blue decays as a function of the detergent composition in the mixed aggregates show only small changes until the total solubilization of the vesicles; i.e., a clear acceleration of all the lifetime distributions is visible only for the mixed micelle sample. This underlines again that the probe is principally sensitive to the appearance of the mixed micelles.

Evolution of the fluorescence decays of laurdan as a function of the mixed lipid-OG micelles composition

In this study, samples corresponding to the micellar domain of the vesicle-to-micelle transition have been preferentially selected because the major changes of laurdan emission spectra are recorded in this part of the transition (Fig. 1 *A*). Nine different mixed micelle samples were selected using the solubilization curve presented in Fig. 1 *B* (samples 5 to 13). The compositions in detergent and lipid of these samples are different because the lipid concentration slightly decreases due to the dilution of the sample induced by the detergent addition whereas the OG concentration increases from 21.5 to 57.9 mM.

For each of these samples, fluorescence decays have been recorded at $\lambda_{exc} = 360$ nm and for two different emission

wavelengths situated in the blue edge (λ_{em} = 400 nm) and in the red edge (λ_{em} = 590 nm) of the spectrum. The results of the MEM analysis are reported on Fig. 4, *A* and *B*, for the blue and red decays, respectively. On these graphs, the results of MEM analysis of laurdan inserted in pure OG micelles have been added for comparison (λ_{exc} = 360 nm and λ_{em} = 600 nm).

The MEM analyses of the red decays all result in two lifetime distributions associated with opposite amplitudes (Fig. 4 *B*). As for the previous samples, the lifetime distributions associated with a negative amplitude reflect the dipolar relaxation process (T_{rel}) whereas the ones associated with a positive amplitude represent the lifetime distribution of the relaxed excited state (τ_{rel}). In Fig. 3 we have reported the evolution of both lifetime distributions with OG concentration: τ_{rel} and T_{rel} are continuously decreasing from 3.9 to 3.2 ns and 1.9 to 1 ns, respectively. It also appears from Fig. 4 *B* that the time distributions associated with the dielectric relaxation process become broader and broader with increasing OG concentration in the mixed micelles and for pure OG micelles.

The results of the MEM analyses of the blue fluorescence decays are complex: three to four lifetime distributions all associated with positive amplitudes are determined as for the samples studied in the previous section (Fig. 4 *A*). Similarly again, a long but weak lifetime distribution can be determined by the MEM analysis on few samples (samples 5, 9, 10, and 11). This distribution may be attributed to τ_{rel}. A very short lifetime distribution (60–70 ps) associated with a strong amplitude is observed. Light scattering generated by the mixed aggregates studied may contaminate this distribution. Indeed, for these experiments, the emission wavelength was settled at 400 nm, the very blue edge of the emission spectra, where the fluorescence signal may be of the same order of magnitude as the signal due to light scattering. However, the different attempts to suppress the signal originating from light scattering did not affect greatly the short distribution observed. This short component of the decay may then result from a combination of light scattering and a real component associated with the fluorescence decay. However, for all the decays analyzed, no clear evolution of the different lifetime distributions with the detergent/lipid ratio of the aggregates can be established.

TRES of laurdan inserted in pure liposomes, mixed micelles, and pure OG micelles

The decays of the previous experiments were recorded in extreme conditions, i.e., in the very blue and very red edges of the emission spectrum of laurdan. The MEM analyses of the decays recorded in the red edge of the emission spectrum clearly show two lifetime distributions respectively related to the relaxation process and the lifetime of the relaxed excited state. An acceleration of these two lifetime distributions is recorded when the detergent concentration is increased, i.e., during the vesicle-to-micelle transition. On the contrary, the analyses of the decays recorded in the blue edge of the emission spectrum indicate a complex de-excitation pathway of the probe that cannot be explained by simple phenomena. Therefore, to understand the transition between these two extreme spectral regions, we determined the time-resolved emission spectra of three different samples, i.e., pure EPC/EPA liposomes, mixed EPC/EPA-OG micelles containing the highest proportion of lipids, and pure OG micelles.

For each of the three types of aggregates, the excitation wavelength was kept constant (360 nm for the pure lipo-
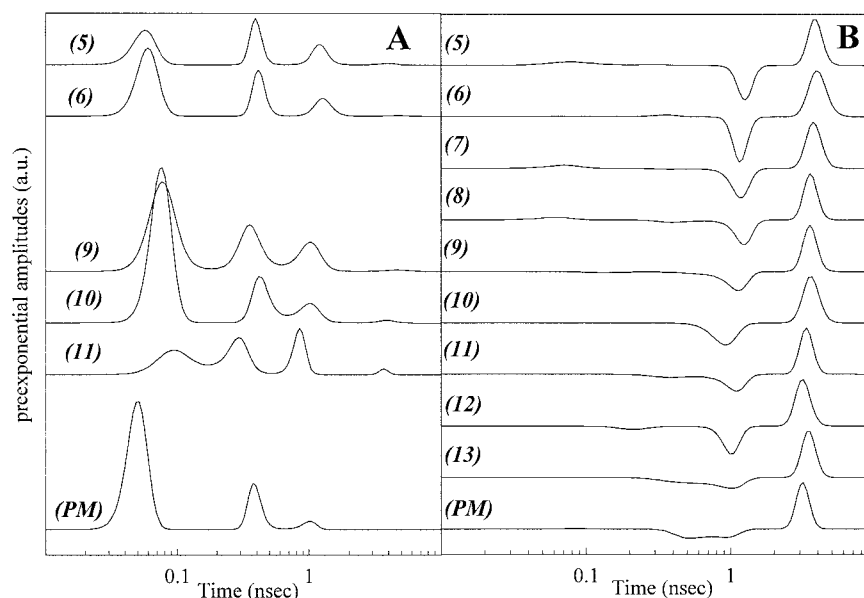

FIGURE 4 Results of the MEM analysis of the fluorescence decays recorded for laurdan inserted in the mixed aggregates indicated on Fig. 1 *B* by the arrows 5 to 13. The sample called PM represents the MEM analysis of laurdan inserted in pure OG micelles ([OG] = 100 mM; [laurdan] = 3 μM). For each sample, the traces on the left are the analysis of the fluorescence decays recorded in the blue edge of the emission spectra (λ_{blue} = 400 nm), whereas the traces on the right are the analysis obtained for the fluorescence decays recorded in the red edge of the spectra (λ_{red} = 590 nm). The excitation wavelength was fixed at 360 nm for all the samples, and the temperature was kept constant at 20°C.

somes and 370 nm for the mixed micelles and for the pure micelles) and the emission wavelengths were selected as indicated in Fig. 5, *A–C*, to describe all the emission spectra of laurdan. The MEM analyses of these decays are reported of Fig. 5, *A–C*, for laurdan inserted in pure liposomes, mixed micelles, and pure micelles, respectively. From those analyses and whatever the aggregate considered, two spectral regions (a blue one and a red one) can be distinguished considering the existence of lifetime distributions associated with negative amplitudes. The wavelength that delimits those two regions depends on the type of aggregate in which laurdan is inserted and increases from 460 nm for pure liposomes to 470 nm for mixed micelles and 480 nm for pure micelles. As expected from the previous results, the fluorescence decays obtained in the blue spectral region are complex, and two to three lifetime distributions all associated with positive amplitudes are determined. In the red spectral region, principally two lifetime distributions associated with opposite-sign amplitudes are determined. The lifetime distributions are almost independent of the emission wavelength. However, as the emission wavelength increases, and especially for laurdan inserted in either pure liposomes or mixed micelles, the proportion of the negative amplitude distribution increases compared with the positive amplitude lifetime distribution. For laurdan inserted in pure micelles, the lifetime distributions associated with negative amplitudes are broader than the ones determined for the two other aggregates.

From the decays analyzed above, the TRES of laurdan inserted in each of the three aggregates studied have been constructed. In Fig. 6, *A–C*, we have reported the TRES normalized in area for laurdan inserted in pure liposomes, in mixed micelles, and in pure micelles, respectively. It appears that the spectra are shifted toward the red whereas their width transiently increases (Figs. 6 and 7). This increase of the spectral width occurs on a time period that depends on the type of aggregate (see Table 1): 5 ns for pure liposomes, 2.3 ns for mixed micelles, and 0.5 ns for pure micelles, indicating an important acceleration of the phenomenon responsible for that pattern. The motion of the emission spectra toward lower-energy regions was followed through the evolution of the barycenters (Fig. 7 *B*), indicating a dissipation of energy of the excited state of laurdan. This dissipation corresponds to a stabilization energy due to reactions occurring with the excited state of laurdan. This stabilization energy (calculated as indicated in the legend of Table 1) depends on the type of aggregate in which laurdan is inserted: 6.55 kcal/mol, 7.06 kcal/mol, and 7.46 kcal/mol for laurdan inserted in pure liposomes, in mixed micelles, and in pure micelles, respectively (see Table 1).

Whatever the type of aggregate, the normalized TRES indicates two different characteristics: the spectra recorded for very short times are shifted toward the red, and for longer times, an isoemissive point is indicated (Fig. 6, *A–C*). The TRES recorded for laurdan in the different aggregates differ only by the rate of their evolution (see Table 1).
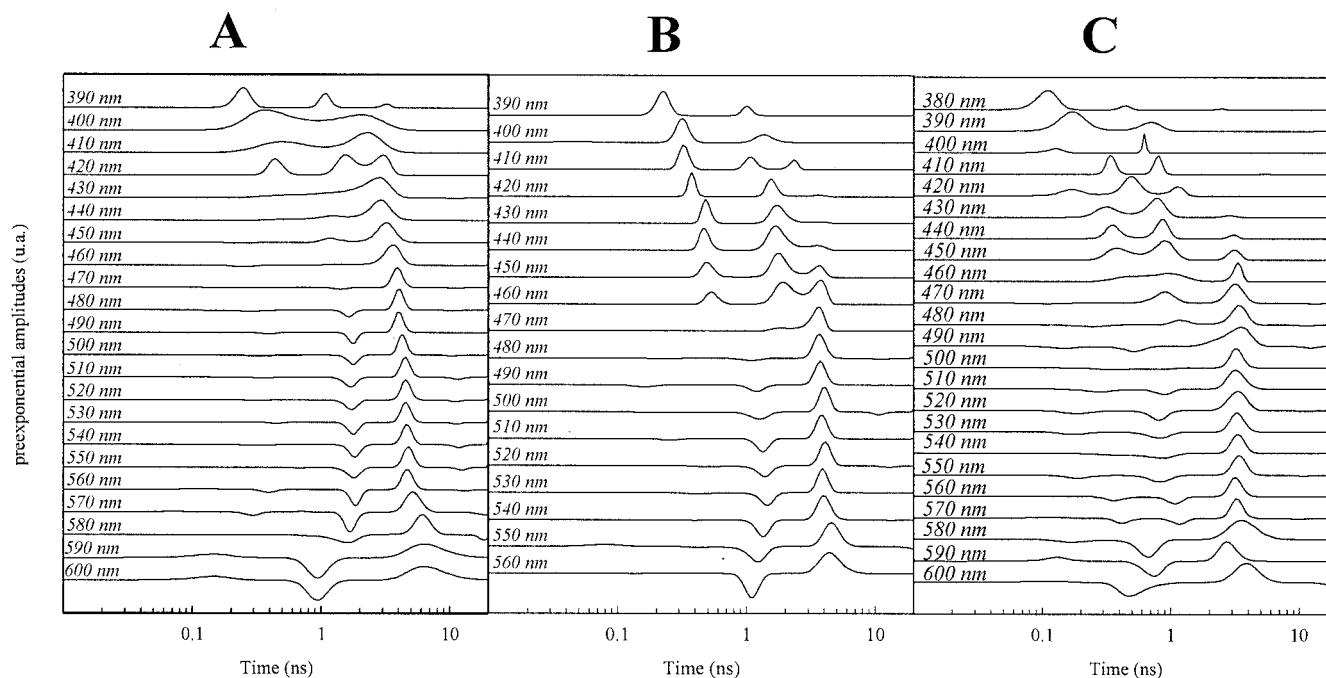

FIGURE 5 Results of the MEM analysis of the fluorescence decays recorded for laurdan inserted in pure EPC/EPA liposomes (*A*), in mixed micelles (point 5 as indicated on Fig. 1 *B* (*B*), and in pure micelle ([OG] = 100 mM; [laurdan] = 3 μM) (*C*). The excitation wavelength was fixed at 360 nm for liposomes and at 370 nm for mixed and pure micelles. The temperature was kept constant at 20°C. The emission wavelengths are indicated on each trace.
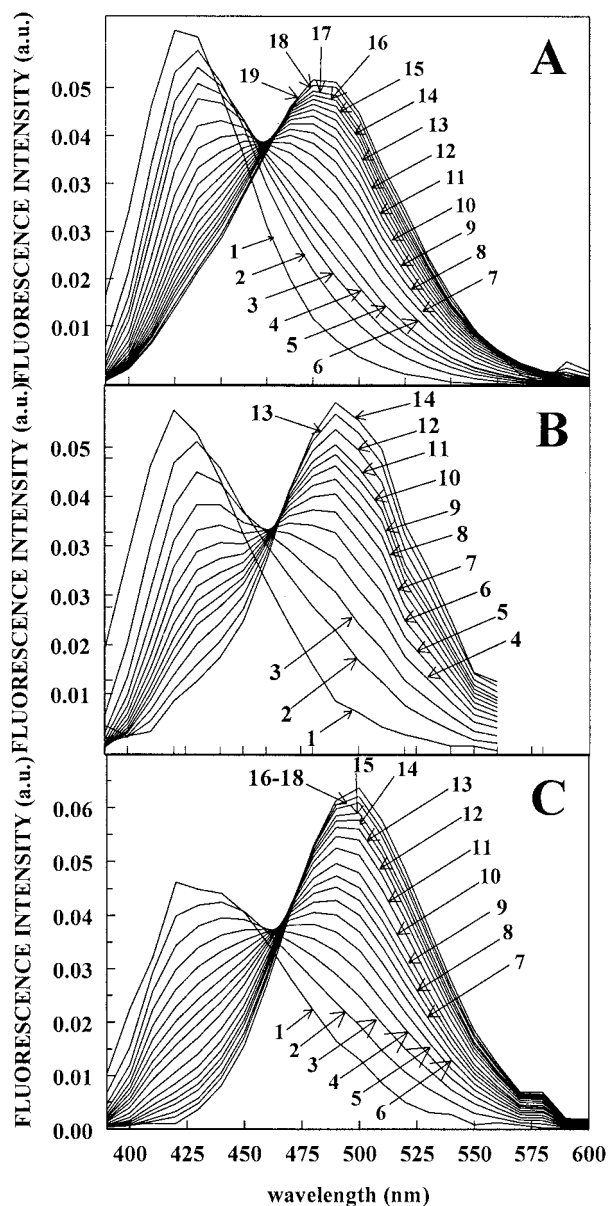
FIGURE 6 TRES of laurdan inserted in pure EPC/EPA liposomes (*A*), in mixed micelles (point 5 as indicated on Fig. 1 *B*) (*B*), and in pure micelle ([OG] = 100 mM; [laurdan] = 3 μM) (*C*). The TRES have been reconstructed by using the results of the MEM analysis illustrated on Fig. 5. The temperature was kept constant at 20°C. (*A*) The spectra were plotted for $t = 0$ (trace 1), $t = 0.5$ ns (trace 2), $t = 1$ ns (trace 3), $t = 1.5$ ns (trace 4), $t = 2$ ns (trace 5), $t = 3$ ns (trace 6), $t = 4$ ns (trace 7), $t = 5$ ns (trace 8), $t = 6$ ns (trace 9), $t = 7$ ns (trace 10), $t = 8$ ns (trace 11), $t = 9$ ns (trace 12), $t = 10$ ns (trace 13), $t = 11$ ns (trace 14), $t = 12$ ns (trace 15), $t = 13$ ns (trace 16), $t = 14$ ns (trace 17), $t = 16$ ns (trace 18), and $t = 18$ ns (trace 19). (*B*) The spectra were plotted for $t = 0$ (trace 1), $t = 0.5$ ns (trace 2), $t = 1$ ns (trace 3), $t = 1.6$ ns (trace 4), $t = 2.2$ ns (trace 5), $t = 2.8$ ns (trace 6), $t = 3.4$ ns (trace 7), $t = 4$ ns (trace 8), $t = 4.6$ ns (trace 9), $t = 5.2$ ns (trace 10), $t = 5.8$ ns (trace 11), $t = 7$ ns (trace 12), $t = 8.8$ ns (trace 13), and $t = 11.2$ ns (trace 14). (*C*) The spectra were plotted for $t = 0$ (trace 1), $t = 0.15$ ns (trace 2), $t = 0.3$ ns (trace 3), $t = 0.45$ ns (trace 4), $t = 0.6$ ns (trace 5), $t = 0.75$ ns (trace 6), $t = 0.9$ ns (trace 7), $t = 1.05$ ns (trace 8), $t = 1.2$ ns (trace 9), $t = 1.4$ ns (trace 10), $t = 1.7$ ns (trace 11), $t = 2$ ns (trace 12), $t = 2.3$ ns (trace 13), $t = 2.6$ ns (trace 14), $t = 2.9$ ns (trace 15), $t = 3.5$ ns (trace 16), $t = 4.1$ ns (trace 17), and $t = 5.9$ ns (trace 18).

DISCUSSION

This aim of this study was to understand the origin of the fluorescence of laurdan and to obtain information about the vesicle-to-micelle transition, and the discussion is constructed around these two different topics.

Conclusion about the origin of laurdan fluorescence in amphiphile aggregates

The MEM analysis of the different fluorescence emission decays pointed out two patterns whatever the aggregate considered. In the higher-energy domain of the emission spectra, complex lifetime distributions associated with positive amplitudes are indicated, whereas in the domain of lower energy, principally two lifetime distributions associated with amplitudes of opposite sign are observed.

Laurdan has been designed to experience an important variation of its dipolar moment upon excitation and thus be very sensitive to its dipolar environment. When inserted in the lipid aggregates, laurdan fluorophore was shown to be located at the level of the phospholipid glycerol backbone. From various studies performed by Parasassi and co-workers, it has been shown that some water molecules present at this level are responsible for the dielectric relaxation observed for laurdan inserted in the fluid lamellar lipid phase. Indeed, the variation of neither the polar headgroup nor the pH influences the emission spectra of laurdan, indicating that the polar headgroups of the lipids are not responsible for this phenomenon (Parasassi et al., 1991). This phenomenon is known to be essential in laurdan photophysics (Viard et al., 1997; Parasassi et al., 1998) and is clearly indicated in this study on the MEM analysis of the fluorescence decays recorded for wavelengths situated in the red part of the emission spectra by the negative amplitude lifetime distribution (T_{rel}). This dielectric relaxation observed for laurdan in amphiphile aggregates is much slower (see Table 1) than dielectric relaxation occurring in bulk water for which rate constants in the picosecond range have been determined. However, if the hydration water is responsible for this phenomenon, its freedom depends on the packing of the molecules forming the structures. Obviously, if the interfacial water is never free in the aggregates studied, its mobility is higher in pure micelles than in vesicles as can be seen from the decrease of T_{rel} from 2.5 to 0.9 ns (Fig. 3). Moreover, in this red spectral region and for all the amphiphile aggregates studied, the unique positive lifetime distribution determined by the MEM analysis of the decays can be unambiguously related to the lifetime of the emissive state originating from that reaction, i.e., the solvent relaxed emissive state (τ_{rel}). The complexity of the time constant distributions obtained in the high-energy domain of the spectra indicates that the solvent relaxation does not account
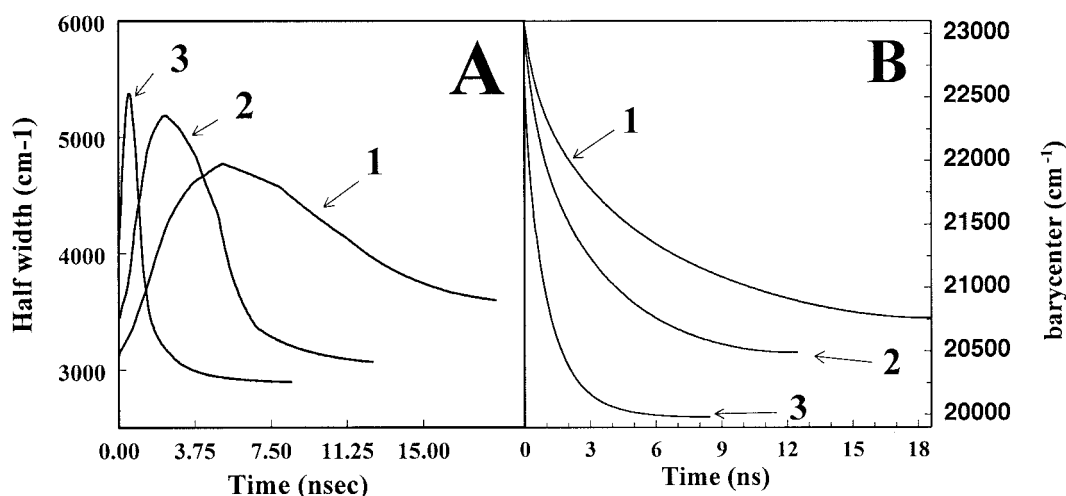
FIGURE 7 Evolution with time of the half width (*A*) and of the barycenters (*B*) of the TRES for laurdan inserted in pure liposomes (traces 1), mixed micelles (traces 2), and pure OG micelles (traces 3).

for all laurdan photophysics, and at least one emissive state should be added to the solvent unrelaxed and relaxed excited states.

To verify the interpretation of the different rate constants determined, we have recorded TRES of laurdan inserted in DPPC liposomes either in a gel or in a fluid lamellar phase (Fig. 8, *A* and *B*). Indeed, the sensitivity of laurdan to the gel-to-fluid lamellar phase transition has been extensively studied and is mainly due to the progressive appearance of the dielectric relaxation process during the lipid phase transition (Parasassi et al., 1986a,b). The TRES of laurdan in DPPC liposomes at 50°C (Fig. 8 *B*), i.e., fluid lamellar phase, is very similar to the TRES obtained for laurdan EPC/EPA liposomes (Fig. 6 *A*). On the contrary, the TRES obtained for laurdan inserted in DPPC gel lamellar phase is very different because only a small red shift of the emission spectra can be seen. The analyses of the evolution of TRES

barycenters (Table 1) show that if the stabilization energy of laurdan in the fluid lamellar phase of DPPC is very similar to that in EPC/EPA liposomes (6.5 kcal/mol and 6.5_5 kcal/mol, respectively), it is much smaller in the gel lamellar phase (1.3 kcal/mol). This difference can be attributed to the appearance of the dielectric relaxation phenomenon occurring during the lipid phase transition. On the other hand, the low stabilization energy of laurdan in the gel lamellar phase may be due to the charge transfer fast reaction. From these last experiments carried on the DPPC system, the complexity of the results given by the MEM analyses of the blue decays for laurdan inserted in amphiphile aggregates can therefore be explained by the existence of a charge transfer fast reaction preceding the solvent relaxation process. The contribution of the solvent relaxation in the blue edge of the emission spectrum is almost negligible because the lifetime distribution associated with the solvent relaxed excited state

TABLE 1 Data obtained from the temporal evolution of the half width and the barycenter of the TRES

Samples	Temporal domains increase of TRES width (ns)	T_{rel}* (ns)	Reaction time constants determined from the MEM analysis of the time-dependent evolution of the barycenter[†]		Stabilization energy[‡] (kcal/mol)
			τ_{r1} (nsec)	τ_{r2} (nsec)	
DPPC liposomes, 20°C			0.3	1.9	1.3
DPPC liposomes, 50°C	2.0	1.8	0.2	1.2	6.5
EPC/EPA liposomes	5.0	2.5	0.2	1.6	6.5_5
Mixed micelles (C point)	2.3	1.9	0.1_5	1.1	7.1
Pure OG micelles	0.5	0.9	0.1	0.8_5	7.5

*For comparison the values of T_{rel} of Fig. 3 are reported.

[†]Reaction rate constants (τ_{rj}) were determined from the analysis of $C(t)$ as a sum of exponentials with MEM (Vincent et al., 1995a, 1995b): $C(t) = \sum_j a_j e^{-t/\tau_{Rj}}$ (Eq. 10).

[‡]ΔE is calculated from the maximal time-dependent shift of the TRES barycenter and is given by $\Delta E = Nhc\Delta\nu$, where N is the Avogadro number, h is the Planck constant expressed in erg-s, and c is the light velocity (cm/s), $\Delta\nu$ is the maximal variation of the time-dependent shift of the TRES barycenters (in cm^{-1}). The energy obtained is given in kcal/mol by using the following energy conversion factor: 1 erg = 2.39 10^{-11} kcal.
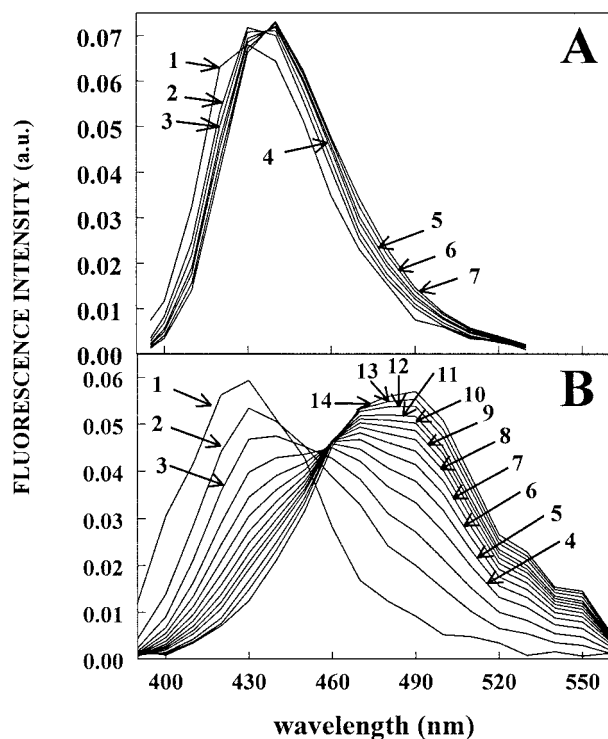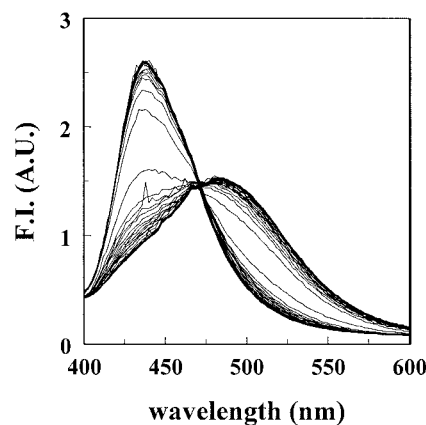
FIGURE 9 Evolution of the steady-state fluorescence spectra of laurdan inserted in DPPC liposomes with temperature. The temperature was increased from 15°C to 65°C at a rate of 0.11°C/min, and the spectra were recorded continuously during the temperature increase. The variation of temperature between the beginning and the end of the spectral acquisition is 0.35°C. The areas of the emission spectra have been normalized.

FIGURE 8 TRES of laurdan inserted in DPPC liposomes in the gel lamellar phase ($T = 20°C$; A) and in the fluid lamellar phase ($T = 50°C$; B). The TRES have been reconstructed by using the results of MEM analysis (data not shown) of the fluorescence decays recorded for different emission wavelengths: from 395 to 490 nm for DPPC gel lamellar phase and from 390 to 560 nm for DPPC fluid lamellar phase ($\lambda_{exc} = 360$ nm). (A) The spectra were plotted for $t = 0$ (trace 1), $t = 0.5$ ns (trace 2), $t = 1$ ns (trace 3), $t = 2$ ns (trace 4), $t = 3$ ns (trace 5), $t = 5.5$ ns (trace 6), and $t = 9$ ns (trace 7). (B) The spectra were plotted for $t = 0$ (trace 1), $t = 0.4$ ns (trace 2), $t = 0.8$ ns (trace 3), $t = 1.3$ ns (trace 4), $t = 1.8$ ns (trace 5), $t = 2.3$ ns (trace 6), $t = 2.8$ ns (trace 7), $t = 3.3$ ns (trace 8), $t = 3.8$ ns (trace 9), $t = 4.3$ ns (trace 10), $t = 4.8$ ns (trace 11), $t = 5.8$ ns (trace 12), $t = 6.8$ ns (trace 13), and $t = 8.8$ ns (trace 14).

is either nonexistent or very low in that energy domain (Figs. 2 and 4).

The evolution of the steady-state emission spectra of laurdan recorded during the vesicle-to-micelle transition (Fig. 1 A) shows that, upon OG addition, the blue part of the spectrum is progressively decreased and that the maximum fluorescence intensity is red shifted. The decrease of the blue part of the emission spectra reflects the acceleration of the dielectric relaxation process whereas the red shift indicates a polarity increase of the laurdan environment. During the gel-to-fluid lamellar phase transition of DPPC such a red shift of the spectra is not recorded. Indeed, in Fig. 9 are reported the area-normalized steady-state emission spectra ($\lambda_{exc} = 360$ nm) of laurdan inserted in DPPC liposomes recorded during a continuous increase of the temperature (from 15°C to 65°C at 0.11°C/min). At low temperature, in the gel lamellar phase, the laurdan spectrum is centered at 435 nm, whereas at high temperature, in the fluid lamellar

phase, it is centered at 500 nm with a shoulder at 435 nm. The spectra of laurdan, between the extreme temperatures, progressively change, exhibiting an isoemissive point at 445 nm. This point is revealed by the area normalization of the spectra, the normalization abolishing the eventual differences in quantum yields of the different emissive states. Such an isoemissive point indicates that the probe is progressively experiencing two different environments as the temperature is increased. The gel environment is characterized by an improbable dielectric relaxation (Fig. 8 A), the lipid packing and the restricted motion of the associated water molecules probably being at the origin of this restriction. During the lipid phase transition, the increase of the surface polar headgroup from 47 Å in the gel phase to 71 Å in the fluid phase (Nagle et al., 1996; Sun et al., 1996), by increasing the freedom of the dipolar molecules, allows the dielectric relaxation to occur. Therefore, if during the gel-to-fluid lamellar phase transition, the molecular packing change is principally involved in the fluorescence changes, for the vesicle-to-micelle transition, an additional phenomenon must be considered, i.e., the polarity increase of the laurdan environment caused by the incorporation of OG within the amphiphile aggregates.

Finally, the multiplicity of the excited-state reactions is evidenced by the MEM analysis of the time evolution of the barycenter of the TRES (Fig. 10). In the fluid lamellar membranes, as in mixed and pure micelles, two time constant distributions are observed (τ_{r1} and τ_{r2}; Table 1). The longer and preponderant one (τ_{r2}; Table 1), ranging from 1.9 ns (for pure liposomes) to 0.8 ns (for pure micelles), can be associated with the solvent relaxation process (T_{rel}; Table 1). It is preceded in all cases by a minor short time distribution (τ_{r1}; Table 1) between 320 ps (for pure liposomes) to
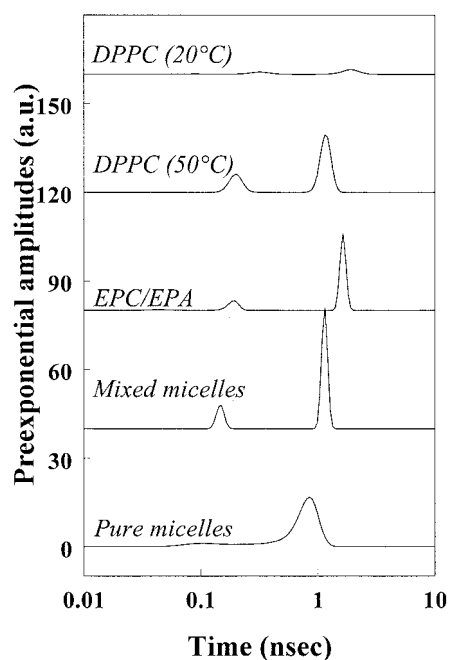
FIGURE 10   MEM analysis of the time evolution of the barycenters of TRES obtained for laurdan inserted in DPPC liposomes at 20°C and 50°C, in EPC/EPA liposomes, in mixed micelles, and in pure OG micelles. The analysis was normalized to the stabilization energy.

114 ps (for pure micelles) that can be related to the charge transfer mechanism.

Therefore, these results support the de-excitation schema proposed by Viard et al. (1997) stating that laurdan de-excitation does not arise from only two emissive states governed only by solvent relaxation processes. In amphiphile aggregates, laurdan fluorescence would arise from at least three different excited states governed by charge transfer and solvent relaxation processes, the rate constant of this last being greatly influenced by the molecular packing of the polar molecules at the interface of the amphiphile aggregates and the polarity of the laurdan environment.

Information obtained from the analysis of laurdan fluorescence on the vesicle-to-micelle transition

Along the vesicle-to-micelle transition, the normalized TRES present the same pattern for all the aggregates (cf. Fig. 6): after a small red shift, an isoemissive point appears. The difference between the aggregates resides in the time constants of the phenomena as it is revealed in Fig. 10 and in the extent of the stabilization energy (Table 1). Interestingly, if τ_{rel} continuously and smoothly decreases all along the transition, T_{rel} is essentially sensitive to the appearance of the first mixed micelle as it can be seen by the breakpoint on the curve relating the evolution of T_{rel} with the total OG concentration in the solution (Fig. 3). The acceleration of the dielectric relaxation concomitantly with the appearance

of the first mixed micelle can be explained by both an increase of the mobility of the interfacial polar molecules and a change in the laurdan environment polarity. Indeed, the increase of the detergent/lipid ratio in the mixed micelles induces an increase of the average curvature radius of the aggregates. This change in curvature radius, by decreasing the packing of the headgroup of the amphiphile, may both facilitate the water molecules' penetration and increase their mobility. Rawat and Chattopadhyay (1999) recently showed that during the sphere-to-rod transition of sodium dodecyl sulfate micelles, N-(-7-nitro-2,1,3-benzoxadiazol-4-yl) fluorophore experiences such changes in its environment polarity when it is located at the micelle interface. In parallel with the acceleration of the relaxation process, a decrease of the lifetime distribution of the relaxed excited state is recorded and may be a consequence of the acceleration of the relaxation rate constant via a dynamic quenching process by water molecules (Stubbs et al., 1995).

The acceleration of the relaxation process is clearly visible for the red decays recorded for laurdan inserted in mixed micelles of increasing detergent/lipid ratio (Fig. 3). In parallel with this acceleration, a broadening of the time distribution associated with the relaxation rate constants by the solvent is recorded (Fig. 4 B). This broadening indicates a heterogeneity of the relaxation time constants that may be due to the properties of the small. globular mixed micelles obtained at high detergent/lipid ratio or for pure micelles. Indeed, the surface of pure micelles is not well defined and is probably rough (Tanford, 1980), implying that lipids and laurdan experience different environments in the same micelle. Because of this undefined surface, water molecules can penetrate at different levels within the micelle.

The increase of the detergent/lipid ratio in the micellar region induces important morphological modifications (Vinson et al., 1989; Edwards et al., 1993; Seras et al., 1996): from elongated mixed micelles at low detergent/lipid ratio to globular ones at high detergent/lipid ratio. Therefore, for laurdan inserted in the mixed micellar region, we could have expected that the de-excitation would arise from at least two relaxed excited states reflecting a high and a low curvature environment. In all the decays recorded, only one relaxation process rate constant and one lifetime of the relaxed state was recorded, signifying that laurdan is preferentially located in the lipid environment of low curvature radius and/or that the proportion of laurdan in the high curvature radius is very small and undetectable. Indeed, if some proportion of the laurdan can accommodate a high curvature region, the dynamic quenching by water molecules will greatly decrease its fluorescence signal. In fact, fluorescence quenching is clearly visualized in steady-state experiments: during the vesicle-to-micelle transition the fluorescence intensity decrease is important (~60%), and we have verified that this quenching was not due to light bleaching in our experimental conditions (data not shown).

Interestingly also, the sensitivity of laurdan to the vesicle-to-micelle transition is especially important in the micellar domain of the transition, whereas when laurdan is inserted in the lamellar part of the transition, only very slight changes are visible (Fig. 2). This could indicate that the incorporation of OG in a lipid bilayer in its fluid lamellar phase does not induce an important modification of the lipid packing and that the membrane can accept as much as 1.5 mol of detergent per mol of lipids before any effects. However, Ollivon et al. (1988) proposed, on the basis of permeability measurements that, before the beginning of the solubilization, pores are formed within the bilayers and stabilized by a detergent edge. Moreover, these pores have been visualized on different detergent and lipid systems by electron cryomicroscopy (Vinson et al., 1989; Seras et al., 1996). The detergent edge requires detergent segregation from the constituting lipid bilayers and would be a region of high curvature radius. As already stated, laurdan does not seem to insert easily in the region of high curvature, or its fluorescence is quenched. Therefore, we have no indication of the existence of these detergent-stabilized pores.

CONCLUSION

The evolution of fluorescence decays of laurdan during the vesicle-to-micelle transition indicates that 1) the packing of the polar headgroups decreases, 2) the environment of the probe becomes more and more polar, and 3) the interface between the water and the aggregates becomes less and less defined. This last point is important to be considered when detergents are used to solubilize membrane proteins. Indeed, if the change in the detergent/lipid/protein ratio modifies not only the shape of the micelle but also the water penetration within the mixed micelle, some hydrophobic parts of the protein may then be exposed to the water originating its denaturation. Therefore, it appears from this study that the size, the shape, and the detergent/lipid composition of the mixed micelle are important parameters to control in order to monitor the solubilization and the conformation of membrane proteins.

REFERENCES

Bagchi, B. 1989. Dynamics of solvation and charge transfer reactions in dipolar liquids. *Annu. Rev. Phys. Chem.* 40:115–141.

Balter, A., W. Nowak, W. Pawelkiewicz, and A. Kowalczyk. 1988. Some remarks on the interpretation of the spectral properties of Prodan. *Chem. Phys. Lett.* 143:565–570.

Chong, P. L.-G. 1988. Effects of hydrostatic pressure on the location of PRODAN in lipid bilayers and cellular membranes. *Biochemistry.* 27: 399–404.

Chong, P. L.-G., S. Capes, and P. T. T. Wong. 1989. Effects of hydrostatic pressure on the location of PRODAN in lipid bilayers: A FT-IR Study. *Biochemistry.* 28:8358–8363.

Chong, P. L.-G., and P. T. T. Wong. 1993. Interactions of Laurdan with phosphatidylcholine liposomes: a high pressure FTIR study. *Biochim. Biophys. Acta.* 1149:260–266.

Cowley, D. J. 1986. Polar pocket with nonpolar lining. *Nature.* 319:14–11.

Edwards, K., J. Gustafsson, M. Almgren, and G. Karlsson. 1993. Solubilization of lecithin vesicles by a cationic surfactant: intermediate structures in the vesicle-micelle transition observed by cryo-transmission electron microscopy. *J. Colloid Interface Sci.* 161:299–309.

Garavito, R. M., D. Picot, and P. J. Loll. 1996. Strategies for crystallizing membrane proteins. *J. Bioenerg. Biomembr.* 28:13–27.

Heerklotz, H., H. Binder, and G. Lantzsch. 1994. Determination of the partition coefficients of the nonionic detergent C12E7 between lipid-detergent mixed membranes and water by means of laurdan fluorescence spectroscopy. *J. Fluoresc.* 4:349–352.

Helenius, A., and K. Simons. 1975. Solubilization of membranes by detergents. *Biochim. Biophys. Acta.* 415:29–79.

Lesieur, S., C. Grabielle-Madelmont, M. Paternostre, and M. Ollivon. 1993. Study of size distribution and stability of liposomes by high performance gel exclusion chromatography. *Chem. Phys. Lipids.* 64: 57–82.

Lichtenberg, D. 1996. Liposomes as a model for solubilization and reconstruction of membranes. *In* Handbook of Nonmedical Applications of Liposomes. Y. Barenholz and D.D. Lasic, editors. CRC Press, Boca Raton, FL. 199–218.

Lichtenberg, D., R. J. Robson, and E. A. Dennis. 1983. Solubilization of phospholipids by detergents. Structural and Kinetic Aspects. *Biochim. Biophys. Acta.* 737:285–304.

Livesey, A. L., and J. C. Brochon. 1987. Analyzing the distribution of decay constants in pulse-fluorimetry using the maximum entropy method. *Biophys. J.* 52:693–706.

Ollivon, M., O. Eidelman, R. Blumenthal, and A. Walter. 1988. Micelle-vesicle transition of egg phosphatidylcholine and octyl glucoside. *Biochemistry.* 27:1695–1703.

Nagle, J. F., R. Zhang, S. Tristan-Nagle, W. Sure, H. I. Petrache, and R. M. Suter. 1996. X-ray structure determination of fully hydrated L_α phase dipalmitoyl phosphatidylcholine bilayers. *Biophys. J.* 70:1419–1431.

Parasassi, T., F. Conti, and E. Gratton. 1986a. Fluorophores in a polar medium: time dependence of emission spectra detected by multifrequency phase and modulation fluorometry. *Cell. Mol. Biol.* 32:99–102.

Parasassi, T., F. Conti, and E. Gratton. 1986b. Time-resolved fluorescence emission spectra of laurdan in phospholipid vesicles by multifrequency phase and modulation fluorometry. *Cell. Mol. Biol.* 32:103–108.

Parasassi, T., G. De Stasio, A. d'Ubaldo, and E. Gratton. 1990. Phase fluctuation in phospholipid membranes revealed by laurdan fluorescence. *Biophys. J.* 57:1179–1186.

Parasassi, T., G. De Stasio, G. Ravagnan, R. M. Rush, and E. Gratton. 1991. Quantitation of lipid phase in phospholipid vesicles by the generalized polarization of laurdan fluorescence. *Biophys. J.* 60:179–189.

Parasassi, T., M. Di Stefano, M. Loiero, G. Ravagnan, and E. Gratton. 1994a. Influence of cholesterol on phospholipid bilayers phase domains as detected by laurdan fluorescence. *Biophys. J.* 66:120–132.

Parasassi, T., M. Di Stefano, M. Loiero, G. Ravagnan, and E. Gratton. 1994b. Cholesterol modifies water concentration and dynamics in phospholipid bilayers: a fluorescence study using laurdan probe. *Biophys. J.* 66:763–768.

Parasassi, T., A. M. Giusti, M. Raimondi, and E. Gratton. 1995. Abrupt modifications of phospholipid bilayer properties at critical cholesterol concentrations. *Biophys. J.* 68:1895–1902.

Parasassi, T., and E. Gratton. 1992. Packing of phospholipid vesicles studied by oxygen quenching of laurdan fluorescence. *J. Fluoresc.* 2:167–174.

Parasassi, T., E. K. Krasnowska, L. Bagatolli, and E. Gratton. 1998. Laurdan and Prodan as polarity-sensitive fluorescent probes. *J. Fluores.* 8:365–373.

Paternostre, M., O. Meyer, C. Grabielle-Madelmont, S. Lesieur, M. Ghanam, and M. Ollivon. 1995. Partition coefficient of a surfactant between aggregates and solution: application to the micelle-vesicle transition of egg-phosphatidylcholine and Octyl-b-D glucopyranoside. *Biophys. J.* 69:2476–2488.

Paternostre, M.-T., M. Roux, and J.-L. Rigaud. 1988. Mechanisms of membrane protein insertion into liposomes during reconstitution procedures involving the use of detergents. I. Solubilization of large unilamellar liposomes (prepared by reverse-phase evaporation) by Triton X-100, octyl glucoside, and sodium cholate. *Biochemistry.* 27: 2668–2677.

Rawat, S. S., and A. Chattopadhyay. 1999. Structural transition in the micellar assembly: a fluorescence study. *J. Fluoresc.* 9:233–244.

Rigaud, J.-L., M.-T. Paternostre, and A. Bluzat. 1988. Mechanisms of membrane protein insertion into liposomes during reconstitution procedures involving the use of detergents. II. Incorporation of the light-driven proton pump bacteriorhodopsin. *Biochemistry.* 27:2677–2688.

Rigaud, J.-L., B. Pitard, and D. Levy. 1995. Reconstitution of membrane proteins into liposomes: application to energy-transducing membrane proteins. *Biochim. Biophys. Acta Bioenerg.* 1231:223–246.

Rottenberg, H. 1992. Probing the interactions of alcohols with biological membranes with the fluorescent probe prodan. *Biochemistry.* 31: 9473–9481.

Schullery, S. E., C. F. Schmidt, P. Felgner, T. W. Tillack, and T. E. Thompson. 1980. Fusion of dipalmitoylphosphatidylcholine vesicles. *Biochemistry.* 19:3919–3923.

Seras, M., K. Edwards, M. Almgren, G. Carlson, M. Ollivon, and S. Lesieur. 1996. Solubilization of non-ionic monoalkyl amphiphile-cholesterol by octyl glucoside: cryo-transmission electron microscopy of the intermediate structures. *Langmuir.* 12:330–336.

Stubbs, C. D., C. Ho, and S. J. Slater. 1995. Fluorescence techniques for probing water penetration into lipid bilayers. *J. Fluoresc.* 5:19–28.

Sun, W. J., S. Tristan-Nagle, R. M. Suter, and J. F. Nagle. 1996. Structure of gel phase saturated lecithin bilayers: temperature and chain length dependence. *Biophys. J.* 71:885–891.

Sylvius, J. R. 1992. Solubilization and functional reconstitution of biomembrane components. *Annu. Rev. Biomol. Struct.* 21:323–348.

Szoka, F., and D. Papahadjopoulos. 1978. Procedure for preparation of liposomes with large internal aqueous space and high capture by reverse phase evaporation. *Proc. Natl. Acad. Sci. U.S.A.* 75:4191–4198.

Tanford, C. 1980. Micelles. *In* The Hydrophobic Effect: Formation of Micelles and Biological Membranes, 2nd ed. Wiley-Interscience, New York. 42–59

Viard, M., M. Vincent, J. Gallay, B. Robert, and M. Paternostre. 1997. Laurdan solvatochromism: solvent dielectric relaxation and intramolecular excited-state reaction. *Biophys. J.* 73:2221–2234.

Vincent, M., J. Gallay, and A. P. Demchenko. 1995a. Solvent relaxation around the excited state of indole: analysis of fluorescence lifetime distributions and time-dependence spectral shifts. *J. Phys. Chem.* 99: 14931–14941.

Vincent, M., J. Gallay, and A. P. Demchenko. 1995b. Solvent relaxation around the excited state of indole: analysis of fluorescence lifetime distributions and time-dependence spectral shifts. *J. Phys. Chem.* 99: 14931–14941.

Vinson, P. K., Y. Talmon, and A. Walter. 1989. Vesicle-micelle transition of phosphatidylcholine and octyl glucoside elucidated by cryo-transmission electron microscopy. *Biophys. J.* 56:669–681.

Wahl, P. 1979. Analysis of fluorescence anisotropy decays by a least square method. *Biophys. Chem.* 91–104.:

Zeng, J. W., and P. L.-G. Chong. 1991. Interactions between pressure and ethanol on the formation of interdigitated DPPC liposomes: a study with prodan fluorescence. *Biochemistry.* 30:9485–9491.